Analysis of slope stability based on evaluation of force balance

A. G. Razdolsky†, D. Z. Yankelevsky‡ and Y. S. Karinski‡†

National Building Research Institute, Technion, Haifa, Israel

Abstract. The paper presents a new approach for the analysis of slope stability that is based on the numerical solution of a differential equation, which describes the thrust force distribution within the potential sliding mass. It is based on the evaluation of the thrust force value at the endpoint of the slip line. A coupled approximation of the slip and thrust lines is applied. The model is based on subdivision of the sliding mass into slices that are normal to the slip line and the equilibrium differential equation is obtained as the slice width approaches zero. Opposed to common iterative limit equilibrium procedures the present method is straightforward and gives an estimate of slope stability at the value of the safety factor prescribed in advance by standard requirements. Considering the location of the thrust line within the soil mass above the trial slip line eliminates the possible development of a tensile thrust force in the stable and critical states of the slope. The location of the upper boundary point of the thrust line is determined by the equilibrium of the upper triangular slice. The method can be applied to any smooth shape of a slip line, i.e., to a slip line without break points. An approximation of the slip and thrust lines by quadratic parabolas is used in the numerical examples for a series of slopes.

Key words: slope stability; slip surface; thrust line; slice; sliding mass.

1. Introduction

The problem of slope stability is commonly solved by assuming a slip line geometry and subdivision of the sliding mass into vertical slices. The problem is statically indeterminate. In early investigations (Fellenius 1936, Janbu 1954, Bishop 1955) not all the equations of equilibrium were simultaneously satisfied. Obviously, some simplifying assumptions are needed to render the problem into a statically determinate problem. Two basic approaches have been proposed by Morgenstern and Price (1965) and by Spencer (1973) which satisfy both, the moment and the force equilibrium conditions. The first method is based on the assumption of the agreed relationship between the lateral thrust and the vertical shear forces on the side face of the slice. According to the most popular Spencer's method, the inclinations of inter-slice forces are defined by arbitrarily chosen coefficients k_i for each inter-slice boundary, and by an angle θ that is common to all slices. The factor of safety F is determined through an iterative process by varying the values of θ and F until the force and the moment equilibrium conditions are satisfied.

---

† PhD, Research Scientist
‡ Professor
‡† PhD, Research Associate, Corresponding author, E-mail: karinski@tx.technion.ac.il

Another approach that assumes the position of the line of thrust had been developed by Janbu (1973). In this method the thrust line is described by a collection of ordinates and inclinations for each slice interface. The equations of horizontal and vertical equilibrium for each slice can be satisfied only by using an iterative procedure.

However, not only the equilibrium and boundary conditions must be satisfied, but also the implied state of stress within the soil mass must be physically acceptable (Morgenstern and Price 1965). It is commonly accepted that soils do not carry tension. For an arbitrarily chosen slip surface and an arbitrarily accepted assumption about the inter-slice forces inclinations it is not possible to ensure that tension will not be developed in the slipping medium. Therefore, in each particular case, one must examine whether tension exists above the slip surface or not. If the thrust line falls beyond the potential sliding mass i.e., it intersects the slip surface, tension will exist within the soil mass, and in that case it must be concluded that the examined slip surface is not valid.

The question of physical correctness of the results obtained by different methods for slope stability analysis is a subject of discussion among researchers. Yang *et al.* (2001) states that "assumptions in traditional limit equilibrium methods lack sound physical basis." Leshchinsky (1990) thinks that "satisfaction of global equilibrium for a sliding body has no guarantee that internal static conditions will be within an acceptable range." Sharma and Moudud (1992) consider the limit equilibrium method as "only a 'tool' for the assessment of the stability of slopes" and recommend "to pay special attention to the results with a view to ensuring that some of the physical assumptions are not grossly violated by the analysis."

In all above methods, the degree of slope stability is evaluated by the magnitude of the factor of safety determined by an iterative process. However, the soil engineer is normally interested in evaluation of the balance between the internal forces which tend to produce failure of slope by sliding soil mass on the one hand and the mobilized resisting shear forces along the slip surface on the other hand. The mobilized resisting forces are calculated for a value of a factor of safety that is prescribed in advance by standard requirements. The forces that tend to move the soil mass, as well as the resisting forces, act in the direction of the tangent to the slip line. Therefore, it is preferable to subdivide the soil mass into slices by sections that are normal to the slip line and to consider force equilibrium in corresponding (normal and tangent) directions. A tendency to moving of the soil mass can be evaluated by an analysis of the lateral thrust forces acting on the corresponding slice side (which are parallel to the above mentioned resistance shear force, that acts on the sliding mass base).

This paper presents a new approach for the stability evaluation of a soil mass slope that is located over a trial smooth slip line with an in advance prescribed factor of safety. The present approach is straightforward and does not need any iterative procedure. The stability analysis is reduced to a numerical solution of the Cauchy problem for the second-order differential equation which is derived from the equilibrium conditions of an infinitesimal slice as defined above. The equation coefficients and, as a result, the solution depends on the parameters of the assumed coupled slip and thrust lines. A thrust line is approximated by the curve, passing through a certain initial point (which is defined by the slip line) and through the slip line endpoint. Thus the thrust line is always located within the potential sliding mass. The assessment of slope stability is based on the analysis of the thrust force at the endpoint of the slip line. The present method allows the analysis of stability of slopes for any smooth shape of the slip surface (not circular only).

In the following examples the slip surface and the thrust lines are approximated by quadratic parabolas. The results obtained by the proposed method are compared with results presented by other authors.

2. The limit equilibrium equations

The potential sliding mass (of a unit thickness) is subdivided into infinitesimal trapezoidal slices, which are normal to the slip line as shown in Fig. 1. A vertical tension crack at the top of the slope is assumed. The thrust line passes within the bounds of the sliding mass. The shape of the first slice at the upper end is triangular. The slope line (external boundary of the slope cross section) and the trial slip line are defined in a Cartesian coordinate system (Fig. 1) by the equations $y = h(x)$ and $y = H(x)$, respectively. The following forces act on an infinitesimal slice, having a width δs (see Fig. 2):

the normal force: $\boldsymbol{E}(s) = E(s)\,\boldsymbol{t}(s)$,

the shear force: $\boldsymbol{T}(s) = -T(s)\,\boldsymbol{n}(s)$,

the weight of the slice: $\Delta\boldsymbol{W}(s) = \Delta W(s)\,[\boldsymbol{t}(s)\sin\alpha - \boldsymbol{n}(s)\cos\alpha]$.

Here bold letters indicate vectors; $\boldsymbol{t}$, $\boldsymbol{n}$ - are tangent and normal unit vectors of the slip line; s - is
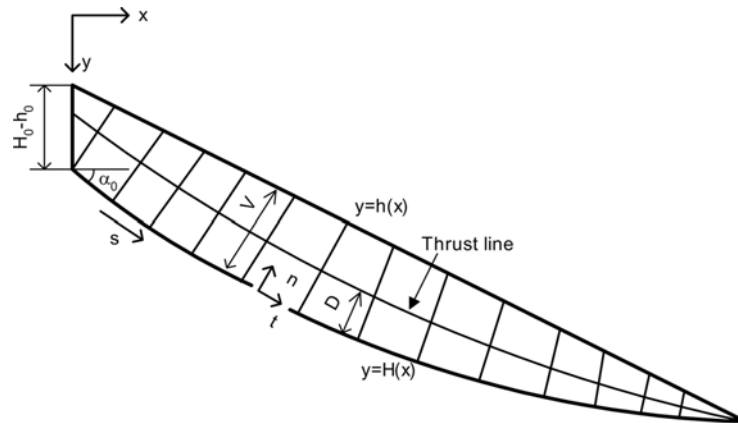

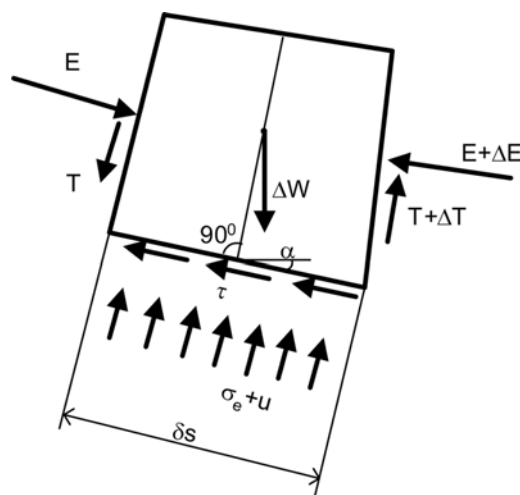Fig. 1 Discretization of the potential sliding mass

Fig. 2 Forces acting on a typical trapezoidal slice

the line coordinate along the slip line, α - is the inclination angle of the slice base (of the slip line at the given point) with respect to the horizontal axis x (see Fig. 1).

Except for the upper triangular slice, all the slices are loaded at their bottom by the effective normal stress $\sigma_e(s)$, the shear stress $\tau(s)$, and the pore water pressure $u(s)$.

The equilibrium of the typical slice leads to the following vector equations:

$$T\left(s - \frac{\delta s}{2}\right) + E\left(s - \frac{\delta s}{2}\right) + \Delta W - T\left(s + \frac{\delta s}{2}\right) - E\left(s + \frac{\delta s}{2}\right) +$$

$$+ \int_{s-\frac{\delta s}{2}}^{s+\frac{\delta s}{2}} \{[\sigma_e(s) + u(s)]n(s) + \tau(s)t(s)\}\,ds = 0 \tag{1}$$

$$\left[R(s) - \left(n(s)\frac{dD(s)}{ds} + D(s)\frac{dn(s)}{ds} + t(s)\right)\frac{\delta s}{2}\right] \times \left[E(s) - \left(\frac{dE(s)}{ds}t(s) + E(s)\frac{dt(s)}{ds}\right)\frac{\delta s}{2}\right] -$$

$$- \left[R(s) + \left(n(s)\frac{dD(s)}{ds} + D(s)\frac{dn(s)}{ds} + t(s)\right)\frac{\delta s}{2}\right] \times \left[E(s) + \left(\frac{dE(s)}{ds}t(s) + E(s)\frac{dt(s)}{ds}\right)\frac{\delta s}{2}\right] -$$

$$- \frac{\delta s}{2}t(s) \times \left[T(s) + \left(n(s)\frac{dT(s)}{ds} + T(s)\frac{dn(s)}{ds}\right)\frac{\delta s}{2}\right] - \tag{2}$$

$$- \frac{\delta s}{2}t(s) \times \left[T(s) - \left(n(s)\frac{dT(s)}{ds} + T(s)\frac{dn(s)}{ds}\right)\frac{\delta s}{2}\right] + \frac{V(s)}{2}n(s) \times \Delta W(s) = 0$$

where $R(s) = D(s)n(s)$ is a vector that passes from the slip line to the thrust line, $V(s)$ is the height of the slice (the depth of the sliding mass) (see Fig. 1), the symbol "$\times$" indicates the vector cross product operation. The weight of the slice is

$$\Delta W = \gamma \int_{s-\frac{\delta s}{2}}^{s+\frac{\delta s}{2}} V(s)\,ds \tag{3}$$

where γ - is the unit weight of the soil mass.

In the above, Eq. (1) expresses the force equilibrium and Eq. (2) expresses the moment equilibrium with respect to the slice base midpoint. The shear stress acting on the slice base in the state of limit equilibrium is defined by the Mohr-Coulomb condition

$$\tau(s) = -\frac{1}{F}[c + \sigma_e(s)\tan\varphi] \tag{4}$$

where c - is the cohesion with respect to the effective stress, φ - is the angle of shearing resistance with respect to the effective stress, F - is the factor of safety.

In the present local coordinate system the unit vectors $t(s)$ and $n(s)$ are related as follows:

$$\frac{dt(s)}{ds} = -\frac{1}{\rho(s)}n(s), \quad \frac{dn(s)}{ds} = \frac{1}{\rho(s)}t(s) \tag{5}$$

where $\rho(s)$ - is the radius of curvature of the slip line at the current point.

Substituting Eqs. (3-5) into (1) and (2) and requiring $\delta s \to 0$ yields the following system of scalar differential equations of equilibrium (the derivations are detailed in Appendix):

$$\frac{dE(s)}{ds} = \gamma V(s)\left(\sin\alpha - \frac{1}{F}\cos\alpha\tan\varphi\right) + \frac{1}{F}\frac{E(s)}{\rho(s)}\tan\varphi + \frac{T(s)}{\rho(s)} + \qquad (6)$$

$$+ \frac{1}{F}\frac{dT(s)}{ds}\tan\varphi - \frac{1}{F}(c - u(s)\tan\varphi)$$

$$T(s) = \gamma\frac{V(s)^2}{2}\sin\alpha - E(s)\frac{dD(s)}{ds} - D(s)\frac{dE(s)}{ds} \qquad (7)$$

Substitution of the shear force (7) into Eq. (6) yields the following equation:

$$\frac{dE(s)}{ds}\left(1 + \frac{D(s)}{\rho(s)}\right) = \gamma V(s)\left[\left(1 + \frac{V(s)}{2\rho(s)}\right)\sin\alpha - \frac{1}{F}\cos\alpha\tan\varphi\right] +$$

$$+ \frac{E(s)}{\rho(s)}\left(\frac{\tan\varphi}{F} - \frac{dD(s)}{ds}\right) + \frac{1}{F}\frac{dT(s)}{ds}\tan\varphi - \frac{1}{F}(c - u(s)\tan\varphi) \qquad (8)$$

The relationships between the line coordinate s and Cartesian coordinates x and y are:

$$\cos\alpha = \frac{dx}{ds} = \frac{1}{\sqrt{1 + \left(\frac{dH}{dx}\right)^2}}, \quad \sin\alpha = \frac{dy}{ds} = \frac{1}{\sqrt{1 + \left(\frac{dH}{dx}\right)^2}}\frac{dH}{dx}$$

$$\frac{1}{\rho(s)} = \frac{1}{\left[1 + \left(\frac{dH}{dx}\right)^2\right]\sqrt{1 + \left(\frac{dH}{dx}\right)^2}}\frac{d^2H}{dx^2} \qquad (9)$$

Substitution of the relationships (9) into the Eqs. (7) and (8) yields following expressions:

$$T = \frac{1}{\sqrt{1 + \left(\frac{dH}{dx}\right)^2}}\left(\frac{1}{2}\gamma V^2\frac{dH}{dx} - E\frac{dD}{dx} - D\frac{dE}{dx}\right) \qquad (10)$$

$$\frac{dE}{dx}\left\{1 + \frac{D\frac{d^2H}{dx^2}}{\left[1 + \left(\frac{dH}{dx}\right)^2\right]\sqrt{1 + \left(\frac{dH}{dx}\right)^2}}\right\} = \gamma V\left\{\left[1 + \frac{V\frac{d^2H}{dx^2}}{2\sqrt{1 + \left(\frac{dH}{dx}\right)^2}\left[1 + \left(\frac{dH}{dx}\right)^2\right]}\right]\frac{dH}{dx} - \frac{\tan\varphi}{F}\right\} -$$

$$- \frac{\tan\varphi}{F}\sqrt{1 + \left(\frac{dH}{dx}\right)^2}\left(\frac{c}{\tan\varphi} - u\right) + \frac{\tan\varphi}{F}\frac{dT}{dx} + \frac{E}{1 + \left(\frac{dH}{dx}\right)^2}\frac{d^2H}{dx^2}\left[\frac{\tan\varphi}{F} - \frac{1}{\sqrt{1 + \left(\frac{dH}{dx}\right)^2}}\frac{dD}{dx}\right] \qquad (11)$$

Therefore, the final form of the differential equation of the slope limit equilibrium becomes:

$$D\frac{d^2E}{dx^2} = E\left\{\frac{\frac{d^2H}{dx^2}}{\sqrt{1+\left(\frac{dH}{dx}\right)^2}}\left[1+\frac{\frac{dH}{dx}-\frac{F}{\tan\varphi}}{\sqrt{1+\left(\frac{dH}{dx}\right)^2}}\frac{dD}{dx}\right]-\frac{d^2D}{dx^2}\right\}-\frac{dE}{dx}\left\{\sqrt{1+\left(\frac{dH}{dx}\right)^2}\frac{F}{\tan\varphi}+2\frac{dD}{dx}+\right.$$

$$\left.+\frac{D\frac{d^2H}{dx^2}}{1+\left(\frac{dH}{dx}\right)^2}\left(\frac{F}{\tan\varphi}-\frac{dH}{dx}\right)\right\}+\gamma V\sqrt{1+\left(\frac{dH}{dx}\right)^2}\left\{\frac{dH}{dx}\left[\frac{F}{\tan\varphi}+\frac{\frac{dV}{dx}}{\sqrt{1+\left(\frac{dH}{dx}\right)^2}}\right]-1\right\}+ \qquad (12)$$

$$+\frac{1}{2}\gamma V^2\frac{d^2H}{dx^2}\left[1+\frac{\frac{dH}{dx}}{1+\left(\frac{dH}{dx}\right)^2}\left(\frac{F}{\tan\varphi}-\frac{dH}{dx}\right)\right]-\left[1+\left(\frac{dH}{dx}\right)^2\right]\left(\frac{c}{\tan\varphi}-u\right)$$

This equation is solved for any given functions $D(x)$, $H(x)$ and $V(x)$ (see Fig. 1).

The parametric form of the equation of the normal to the slip line is:

$$X = x + m\sin\alpha, \quad Y = y - m\cos\alpha \qquad (13)$$

where $\sin\alpha$ and $\cos\alpha$ are calculated by (9) and m - is a variable parameter. Therefore $V(x)$ satisfies the following equation:

$$y - V\cos\alpha = h(x + V\sin\alpha) \qquad (14)$$

In the general case this equation may be solved using numerical techniques. Assume that the slope line is linear, i.e.,

$$\frac{dh(x)}{dx} = k = \text{const} \qquad (15)$$

In that case the solution of (14) is obtained in the explicit form as follows:

$$V(x) = \frac{H(x)-h(x)}{k\frac{dH(x)}{dx}+1}\sqrt{1+\left(\frac{dH(x)}{dx}\right)^2} \qquad (16)$$

Using Eq. (16) and the expression for the pore water pressure: $u(x) = r_u\gamma[H(x)-h(x)]$, where r_u - is the pore water coefficient, Eq. (12) is reduced to the form

$$D\frac{d^2E}{dx^2} = E\left\{ \frac{\dfrac{d^2H}{dx^2}}{\sqrt{1+\left(\dfrac{dH}{dx}\right)^2}}\left[1+\frac{\dfrac{dH}{dx}-\dfrac{F}{\tan\varphi}}{\sqrt{1+\left(\dfrac{dH}{dx}\right)^2}}\frac{dD}{dx}\right] - \frac{d^2D}{dx^2}\right\} - \frac{dE}{dx}\left[\sqrt{1+\left(\frac{dH}{dx}\right)^2}\frac{F}{\tan\varphi}+\right.$$

$$\left. +2\frac{dD}{dx}+\frac{\dfrac{F}{\tan\varphi}-\dfrac{dH}{dx}}{1+\left(\dfrac{dH}{dx}\right)^2}D\frac{d^2H}{dx^2}\right] + \gamma\frac{H-h}{k\dfrac{dH}{dx}+1}\left[1+\left(\frac{dH}{dx}\right)^2\right]\left\{\frac{dH}{dx}\left[\frac{\dfrac{dH}{dx}-k}{k\dfrac{dH}{dx}+1}+\frac{F}{\tan\varphi}\right]-1\right\} + \quad (17)$$

$$+\frac{\gamma}{2}\frac{d^2H}{dx^2}\left(\frac{H-h}{k\dfrac{dH}{dx}+1}\right)^2\left[\frac{F}{\tan\varphi}\frac{dH}{dx}+\frac{1-k\dfrac{dH}{dx}+2\left(\dfrac{dH}{dx}\right)^2}{k\dfrac{dH}{dx}+1}\right] - \left[1+\left(\frac{dH}{dx}\right)^2\right]\left[\frac{c}{\tan\varphi}-r_u\gamma(H-h)\right]$$

Suppose that the slip line upper boundary point is on the slope line: $H(0) = 0$. The following initial conditions must fulfill at that point:

$$E(0) = 0, \quad H(0) = h(0), \quad D(0) = 0, \quad \left(\frac{dD}{dx}\right)_{x=0} > 0 \qquad (18)$$

and from Eq. (17) the following inequality is derived:

$$\left(\frac{dE}{dx}\right)_{x=0} = -\frac{1+\left(\dfrac{dH}{dx}\right)^2}{\sqrt{1+\left(\dfrac{dH}{dx}\right)^2}\dfrac{F}{\tan\varphi}+2\dfrac{dD}{dx}}\frac{c}{\tan\varphi} < 0 \qquad (19)$$

It implies that there exists tension at the initial point. It is commonly accepted that soils do not carry tension, therefore, in fact, the slip line should start only from a bottom of certain tension crack at the slope upper point $x = 0$ (see Fig. 1). It should be mentioned that earlier works found it necessary to introduce a tension crack in order to obtain a statically admissible solution (Spencer 1973, Janbu 1973, Leshchinsky 1990, Sharma and Moudud 1992).

For further analysis of the problem, the following non-dimensional parameters are introduced:

$$\xi = \frac{x}{L}, \quad Y = \frac{H}{L}, \quad Z = \frac{h}{L}, \quad \Omega = \frac{E}{\gamma L^2}, \quad \Lambda = \frac{D}{L}, \quad c_* = \frac{c}{\gamma L\tan\varphi} \qquad (20)$$

where L - is some basic linear dimension, for example, the slope height. Using these parameters, Eq. (17) takes the form

$$\Lambda\Omega'' = -\Omega'\left(\frac{F}{\tan\varphi}\sqrt{1+Y'^2}+\frac{\dfrac{F}{\tan\varphi}-Y'}{1+Y'^2}Y''\Lambda+2\Lambda'\right) + \Omega\left[\frac{Y''}{\sqrt{1+Y'^2}}\left(1+\frac{Y'-\dfrac{F}{\tan\varphi}}{\sqrt{1+Y'^2}}\Lambda'\right)-\Lambda''\right] - $$

$$-(1 + Y'^2)[c_* - r_u(Y - Z)] + \frac{Y - Z}{kY' + 1}(1 + Y'^2)\left[Y'\left(\frac{F}{\tan\varphi} + \frac{Y' - k}{kY' + 1}\right) - 1\right] +$$

$$+ \frac{1}{2}\left(\frac{Y - Z}{kY' + 1}\right)^2 Y''\left(\frac{F}{\tan\varphi}Y' + \frac{1 - kY' + 2Y'^2}{kY' + 1}\right) \tag{21}$$

Here the primes denote the derivatives with respect to the non-dimensional coordinate ξ.

Eq. (21) yields the distributions of the non-dimensional inter-slice lateral thrust force $\Omega(\xi)$ for any given smooth shape of the coupled slip $Y(\xi)$ and thrust $\Lambda(\xi)$ lines and for any given initial conditions.

3. Equilibrium of the initial upper slice

The upper triangular slice that was mentioned in the previous section with the forces acting on it is shown in Fig. 3. In the following solution the assumption (15) of a linear slope line is adopted. Here the vertex O is the upper boundary point of the slip line and α_0 - is the upper end angle of the slip line inclination. The slice side OA (of the length $H_0 - h_0$) coincides with the vertical crack, the side AB lies on the slope line and the slice side OB is normal to the slip line at its upper boundary point. The line segment OM is a median passing through the vertex O. The input geometry parameters (see Figs. 1, 3) are the following:

$$H_0 = H(0), \quad h_0 = h(0), \quad \alpha_0 = \arctan\left(\frac{dH}{dx}\right)_{x=0}, \quad \delta = \arctan(k) \tag{22}$$

The slice weight

$$\Delta W_0 = \gamma\left(\frac{\frac{dH}{dx}}{1 + k\frac{dH}{dx}}\right)_{x=0} (H_0 - h_0)^2 \tag{23}$$
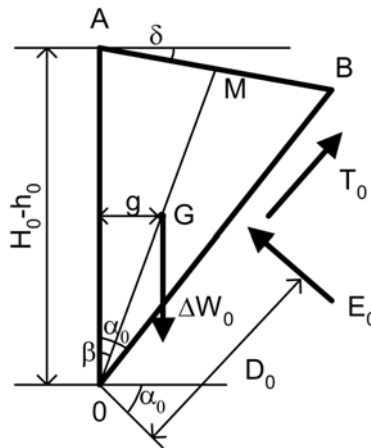

Fig. 3 Forces acting on the upper triangular slice

is applied at the midpoint G of the median and its distance to the side OA is

$$g = \left(\frac{\frac{dH}{dx}}{1 + k\frac{dH}{dx}} \right)_{x=0} \frac{H_0 - h_0}{3} \tag{24}$$

The inter-slice lateral force, which is normal to the side OB, is obtained by the force equilibrium condition

$$E_0 = \Delta W_0 \sin\alpha_0 = \gamma \frac{\left(\frac{dH}{dx}\right)^2}{\left(1 + k\frac{dH}{dx}\right)\sqrt{1 + \left(\frac{dH}{dx}\right)^2}}(H_0 - h_0)^2 \tag{25}$$

The distance D_0 from the upper boundary point of the slip line to the upper boundary point of the thrust line is obtained by the moment equilibrium condition with respect to the vertex point O as follows:

$$D_0 = g\frac{\Delta W_0}{E_0} = \frac{\sqrt{1 + \left(\frac{dH}{dx}\right)^2}}{1 + k\frac{dH}{dx}}\frac{H_0 - h_0}{3} \tag{26}$$

The x-coordinate of the force point of application E_0 is:

$$x_* = D_0 \sin\alpha_0 = \frac{\frac{dH}{dx}}{1 + k\frac{dH}{dx}}\frac{H_0 - h_0}{3} \tag{27}$$

A non-dimensional form of relations (25-27) is obtained by using (20) as follows:

$$\Omega_0 = (Y_0 - Z_0)^2 \frac{Y_0'^2}{(1 + kY_0')\sqrt{1 + Y_0'^2}}$$

$$\Lambda_0 = \frac{\sqrt{1 + Y_0'^2}}{1 + kY_0'}\frac{Y_0 - Z_0}{3}, \quad \xi_* = \frac{Y_0'}{1 + kY_0'}\frac{Y_0 - Z_0}{3} \tag{28}$$

where

$$\xi_* = x_*/L, \quad Y_0 = Y(0), \quad Z_0 = Z(0), \quad Y_0' = Y'(0), \quad \Omega_0 = \Omega(0), \quad \Lambda_0 = \Lambda(0) \tag{29}$$

The values of (28) are used as the upper boundary conditions for Eq. (21). A similar type of a slice was considered by Zhu and Qian (2000) in studying the problem of passive earth pressure analysis.

4. Analysis of the slope stability

In the conventional limit equilibrium procedure, a factor of safety is obtained from the solution with respect to the chosen slide line. In the present approach the factor of safety is prescribed in advance to ensure the slope reliability and the slope stability is evaluated for the assumed coupled slip and thrust lines. The analysis of slope stability is based on the solution of Eq. (21), which may be obtained numerically for any given functions $Y(\xi)$ and $\Lambda(\xi)$. The endpoint coordinate $\xi = \xi_e$ of the slip line is obtained from the slope and slip lines intersection condition:

$$Y(\xi_e) = Z(\xi_e) \tag{30}$$

The boundary conditions at the upper boundary point are calculated according to Eq. (28), the initial value of the derivative is $\Omega' = \Omega'_0$ assumed and Eq. (21) is solved in the range $\xi_0 \le \xi \le \xi_e$. Finally, the non-dimensional force $\Omega(\xi_e) = \Omega_e$ at the endpoint of the slip line is obtained.

The following condition shows that the sliding mass of the slope is in a state of limit equilibrium:

$$\Omega_e = 0 \tag{31}$$

The critical state is defined by the given slip and coupled thrust lines and by the prescribed factor of safety. If the active force is smaller than the slip resistance, the analyzed soil mass is in a stable state and

$$\Omega_e < 0 \tag{32}$$

A criterion for the unstable state of the potential sliding mass is

$$\Omega_e > 0 \tag{33}$$

Such a criterion was applied in Ginzburg and Razdolsky (1992) while solving the slope stability problem using simplified equilibrium equations. A similar approach was used in Takuo *et al.* (2000) for a design method of slopes with a row of piles to enhance the slope stability.

The present method is applicable to any shape of a slip line. For the following analysis the simplest approximation (34) of the slip line by a quadratic parabola is used. In this case the only three parameters of the slip line must be defined in advance: its upper boundary point, its inclination at this point and its endpoint.

$$Y(\xi) = Y(0) + \xi\left(\frac{dY}{d\xi}\right)_{\xi = 0} + \kappa_Y \xi^2 \tag{34}$$

Here:

$$\kappa_Y = \frac{Z(\xi_e) - Y(0) - \xi_e \tan \alpha_0}{\xi_e^{\,2}} \tag{35}$$

The coupled thrust line is expressed by the following quadratic parabola:

$$\Lambda(\xi) = \Lambda(\xi_0) + \xi\left(\frac{d\Lambda}{d\xi}\right)_{\xi = 0} + \kappa_\Lambda \xi^2 \tag{36}$$

An upper boundary point of the thrust line is given by (28). A starting angle θ_0 of the line $\Lambda(\xi)$ is defined by the condition of coincidence of the slip line and thrust line endpoints:

$$\Lambda(\xi_e) = 0 \tag{37}$$

Therefore, the angle θ_0 and the coefficient κ_Λ are given as follows:

$$\theta_0 = \text{atan}\left(\frac{d\Lambda}{d\xi}\right)_{\xi = \xi_0}, \quad \kappa_\Lambda = -\frac{\Lambda(\xi_0) + \xi_e \tan\theta_0}{\xi_e^2} \tag{38}$$

Note that the coupled approximation of the slip and thrust lines excludes the possible development of tension between slices in the stable and critical states of slope.

The proposed method consists in estimation of slope stability at the prescribed normative value of the safety factor $[F]$ and is reduced to a search of a slip line which gives the least stability reserve i.e., the greatest value $\tilde{\Omega} = \max\Omega_e$. The determination of value Ω_e for each step of search of maximum $\tilde{\Omega}$ follows the straightforward method i.e., an iterative process is not needed. The condition of the critical state is $\tilde{\Omega} = 0$.

5. Examples

To evaluate the proposed method of analysis, several examples are illustrated. Quadratic parabola slip and thrust lines are assumed. The first three examples (Figs. 4-6) are intended to demonstrate how the positions of the trial slip and thrust lines affect the stability of the soil mass above the slip line. The chosen slope parameters are identical to those reported by Spencer (1973):

$$\varphi = 30^\circ, \quad k = 1/2.82, \quad c_* = 0.0452/\tan\varphi, \quad r_u = 0$$

The non-dimensional depth of the vertical crack at the slope top is $Y_0 - Z_0 = 0.15$ and the
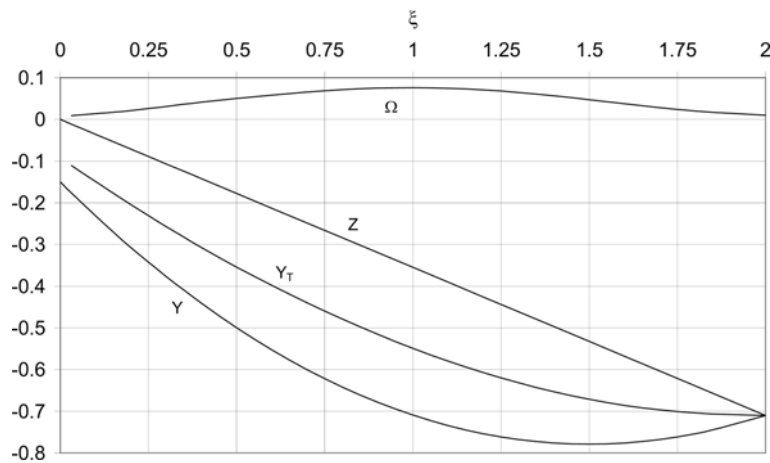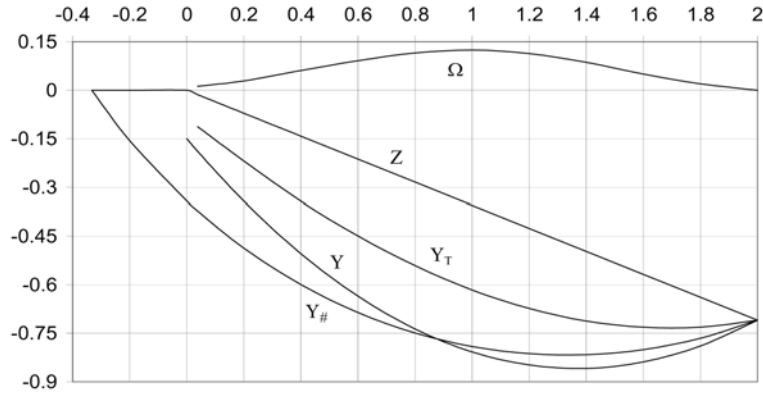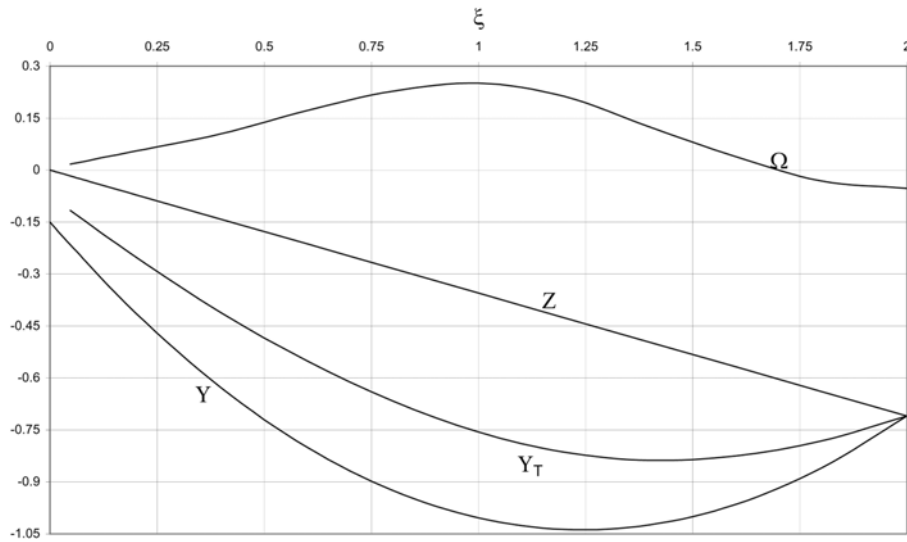

Fig. 4 Thrust force distribution within a soil mass in an unstable state ($\Omega_e > 0$)

Fig. 5 Thrust force distribution within a soil mass in a critical state ($\Omega_e = 0$)

Fig. 6 Thrust force distribution within a soil mass in a stable state ($\Omega_e < 0$)

prescribed factor of safety is $F = 2.7$. Each figure shows the slope line Z, the trial slip line $Y(\xi)$ and the location of the thrust line $Y_T(\xi)$ within the slope as well as the distribution of the thrust force $\Omega(\xi)$. In Fig. 4 that corresponds to an initial angle $\alpha_0 = 40^0$ the final boundary thrust value is $\Omega_e = 0.001 > 0$ and therefore the soil mass can slide along the trial slip line. The thrust distribution in Fig. 5 ($\alpha_0 = 46^0$) corresponds to the critical state of the soil mass: $\Omega_e = 0$ (the feasible slip line). Here the circular slip line $Y_{\#}(\xi)$ considered by Spencer (1973) is also shown. The factor of safety obtained by Spencer for this line is $F = 2.5$. The final boundary thrust value in Fig. 6 ($\alpha_0 = 55^0$) is $\Omega_e = -0.053 < 0$ and therefore the soil mass can not slide along the trial line. A graphical comparison of the above trial slip lines and the thrust force distributions is shown in Fig. 7. The initial angle of inclination α_0 for each trial slip line is indicated.

The value of the factor of safety essentially influences the thrust force distribution and thus the stability evaluation of the soil mass laying above the trial slip line. The influence of the factor of
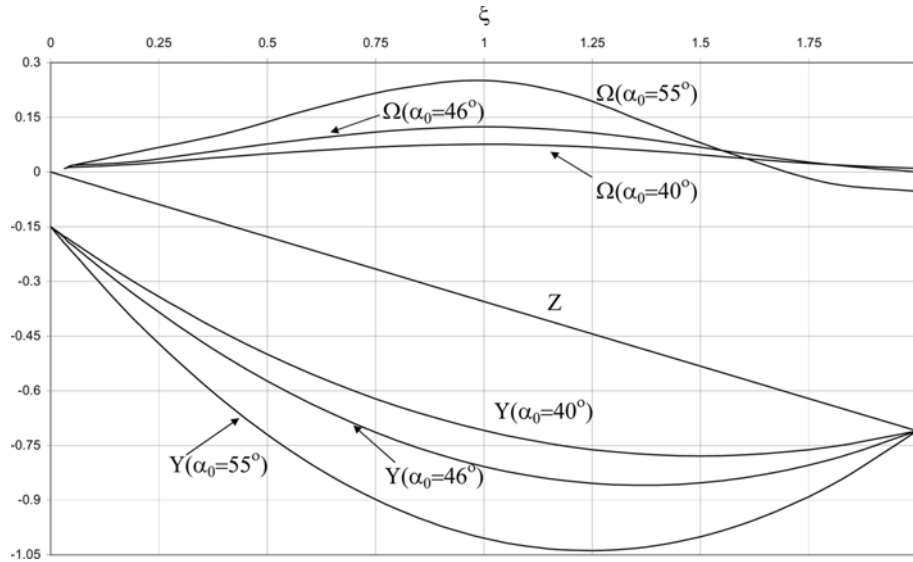
Fig. 7 Comparison of slip line configurations and thrust force distributions for stable, critical and unstable states of a soil mass
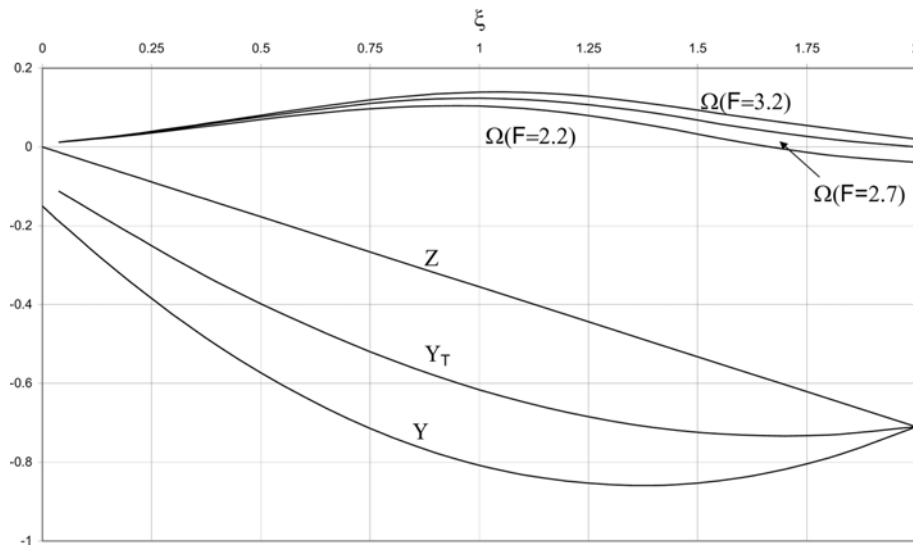
Fig. 8 Influence a safety factor on a thrust force distribution

safety on the thrust force distribution is illustrated in Fig. 8, which corresponds to the initial slip line inclination $\alpha_0 = 46^0$ (see also Fig. 5). The value of $F = 2.2$ yields $\Omega_e = -0.039 < 0$ and corresponds to a stable state of the soil mass. Increasing the factor of safety leads to decrease in stability of the soil mass above the trial slip line. The value of $F = 2.7$ corresponds to the critical state of the soil mass ($\Omega_e = 0$) and $F = 3.2$ yields $\Omega_e = 0.02 > 0$ and corresponds to an unstable state. The feasible slip lines corresponding to the critical states of the slope for the above mentioned values of the safety factors are plotted in Fig. 9. A geometry arrangement of the slip lines shows

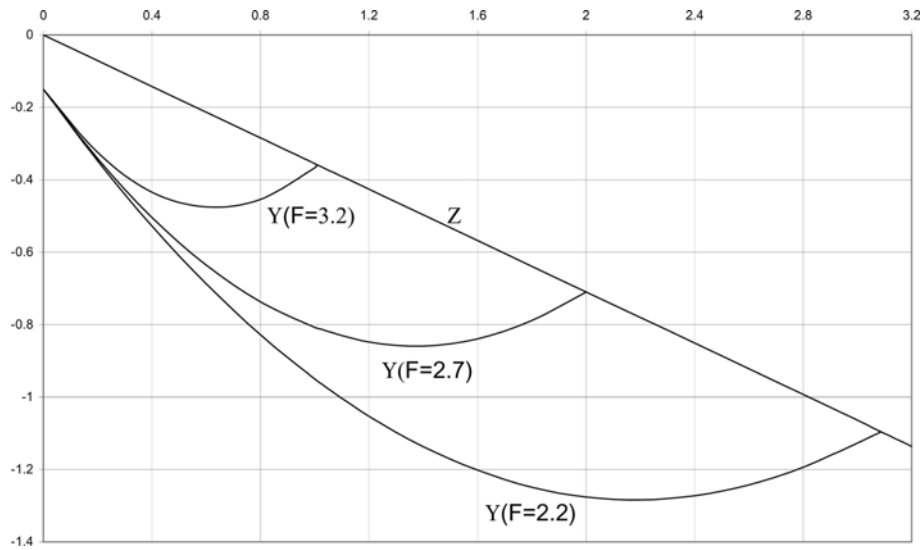Fig. 9 Feasible slip lines corresponding to different values of a safety factor
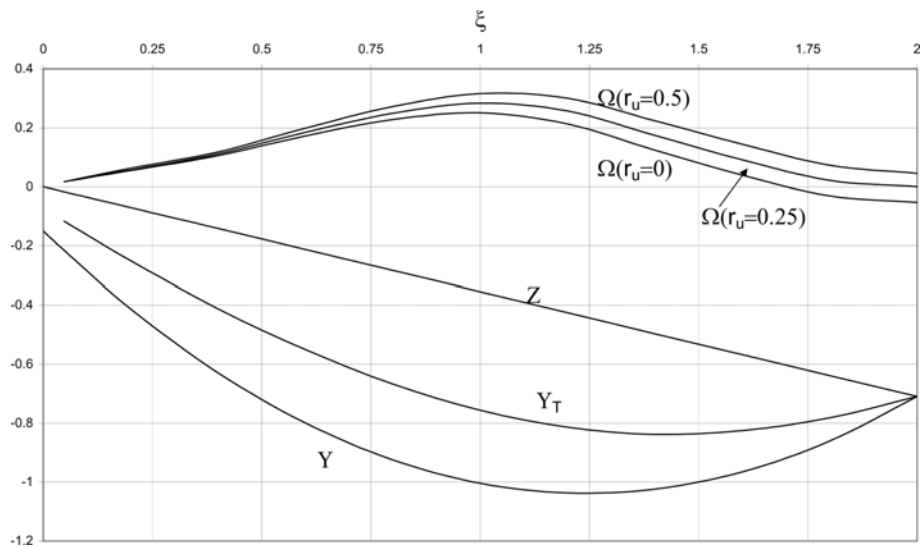
Fig. 10 Influence a pore water pressure on a thrust force distribution

that decreasing the factor of safety leads to increasing the bulk of the sliding mass above the corresponding slip line.

The thrust force distribution and the soil mass above the trial slip line depend on the magnitude of the pore water pressure. Fig. 10 shows the influence of the pore water pressure on the soil mass stability. The slip and thrust lines in this figure are the same as these shown in Fig. 6, and the prescribed factor of safety is $F = 2.7$. Increasing of pore water pressure leads to slope instability. For the pore water coefficient $r_u = 0$ the trial line was found to be stable ($\Omega_e = -0.053 < 0$). The values of the pore water coefficient $r_u = 0.25$ and $r_u = 0.5$ yield $\Omega_e = 0$ (the critical state) and $\Omega_e = 0.045$ (an unstable state), respectively. The feasible slip lines corresponding to the critical states of
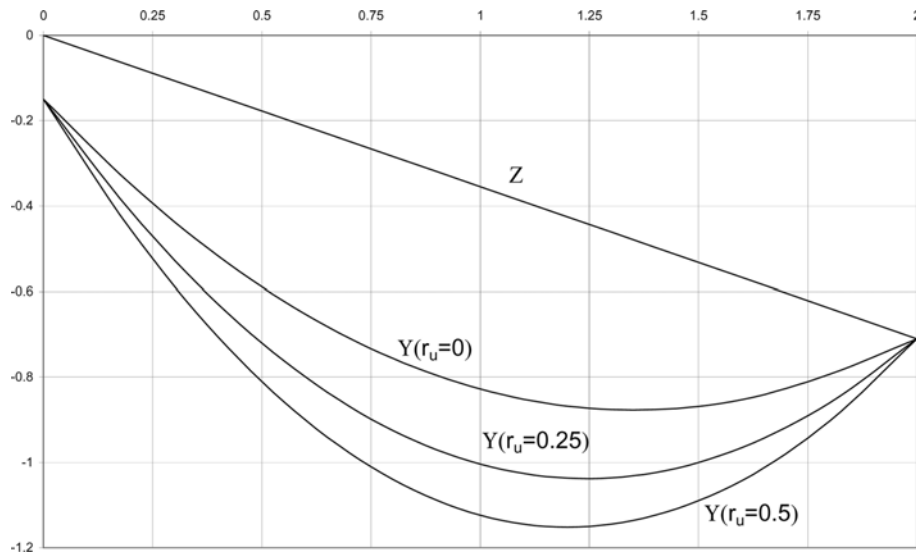
Fig. 11 Feasible slip lines corresponding to different values of a pore water pressure
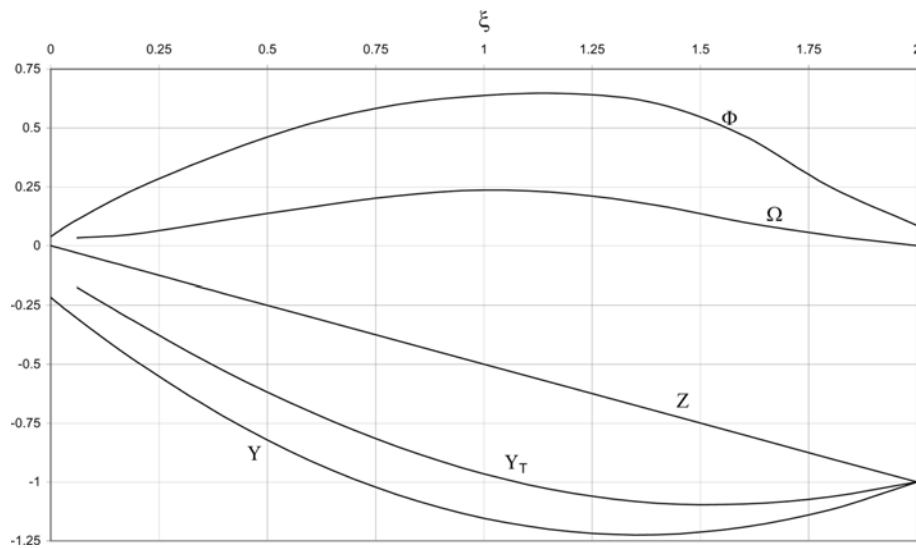
Fig. 12 Thrust force and normal stress distributions corresponding to the critical state of a soil mass, the crack depth is $Y_0 - Z_0 = 0.217$

the slope for the above values of the pore water coefficient are plotted in Fig. 11. They all have common upper and lower boundary points. A geometrical observation of the slip lines shows that increasing the pore water coefficient leads to an increasing sliding soil mass above the corresponding slip line.

Slopes with a crack near the slope upper end were discussed in (Leshchinsky 1990, Sharma and Moudud 1992). The soil parameters were chosen as follows: $\gamma = 110$ pcf, $c = 1000$ pcf, $\varphi = 15^{\rm o}$. The vertical distance from the soil surface to the upper boundary point of the slip line is $H_0 - h_0 = 6.5$
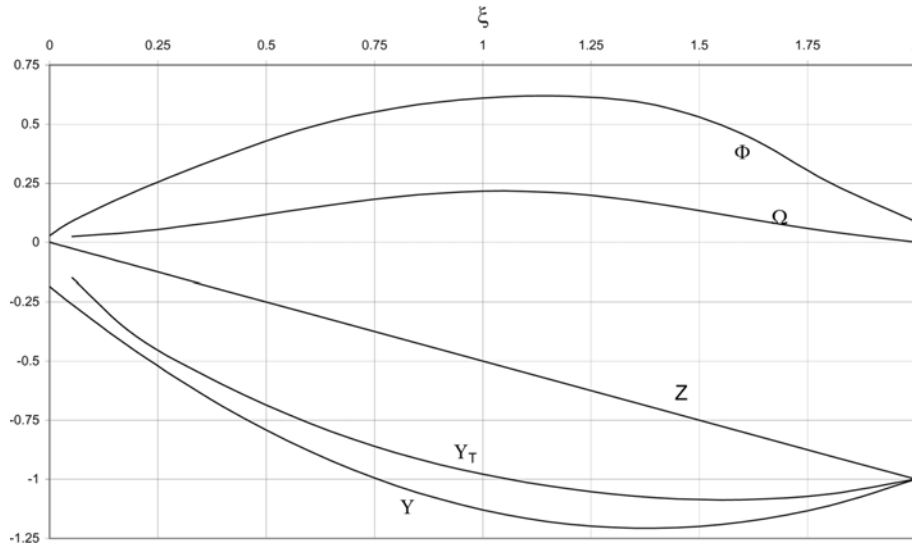
Fig. 13 Thrust force and normal stress distributions corresponding to the critical state of a soil mass for the minimum value of crack depth $Y_0 - Z_0 = 0.185$
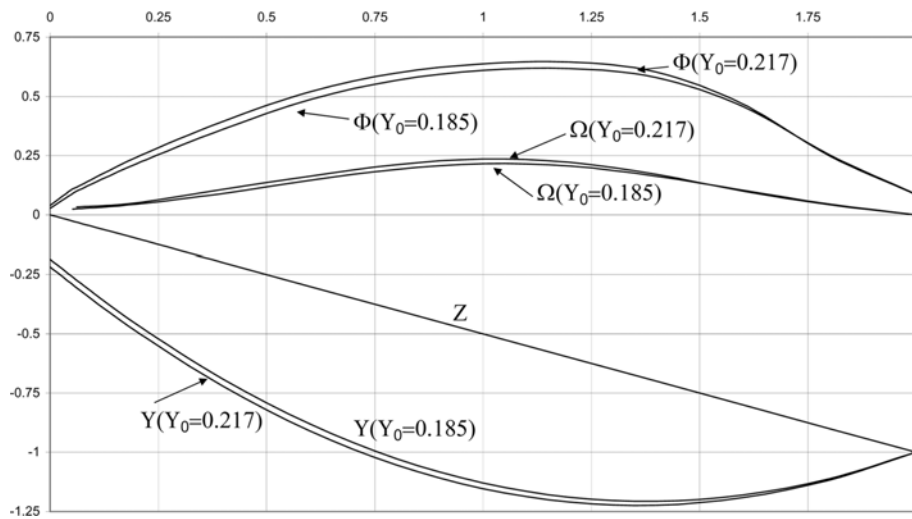
Fig. 14 Comparison of slip line configurations and thrust force and normal stress distributions corresponding to different values of the crack depth

feet (the non-dimensional distance is $Y_0 - Z_0 = 0.217$) and the slope inclination is $k = 0.5$. The plots of the slip and thrust lines, as well as distribution of the thrust force Ω and distribution of the normal stress along the slip line ($\Phi = \sigma_e / \gamma L$) are shown in Fig. 12. The minimum value of the factor of safety is the same as has been obtained in Sharma and Moudud (1992): $F = 2.9$. Fig. 13 shows the results of the slope stability analysis for the slope with the minimal feasible depth of the crack, which was obtained by the proposed method, that equals to $Y_0 - Z_0 = 0.185$. In this case the minimum factor of safety is $F = 3.0$. The slip lines, the thrust force Ω and the normal stress Φ distributions for both cases are shown in Fig. 14. One can see that the differences are negligible.
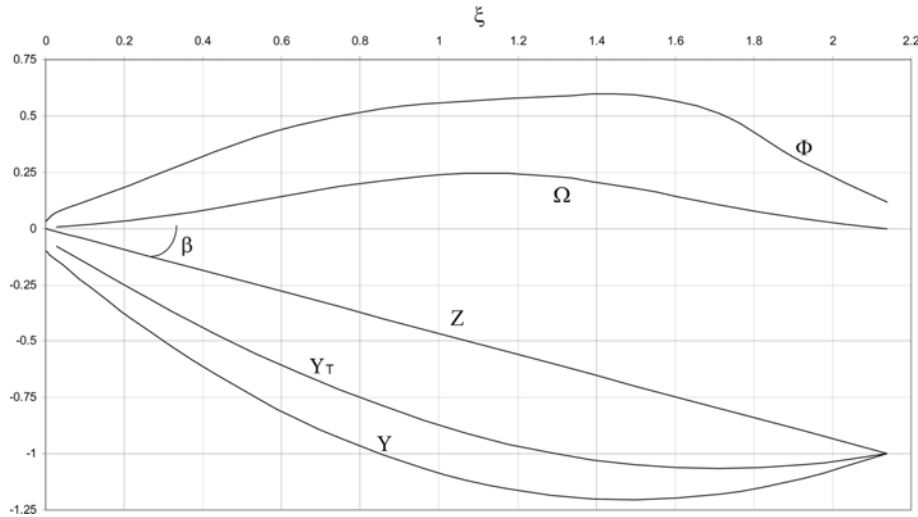
Fig. 15 Thrust force and normal stress distributions corresponding to the minimum value of a safety factor, slope angle inclination $\beta = 25°$
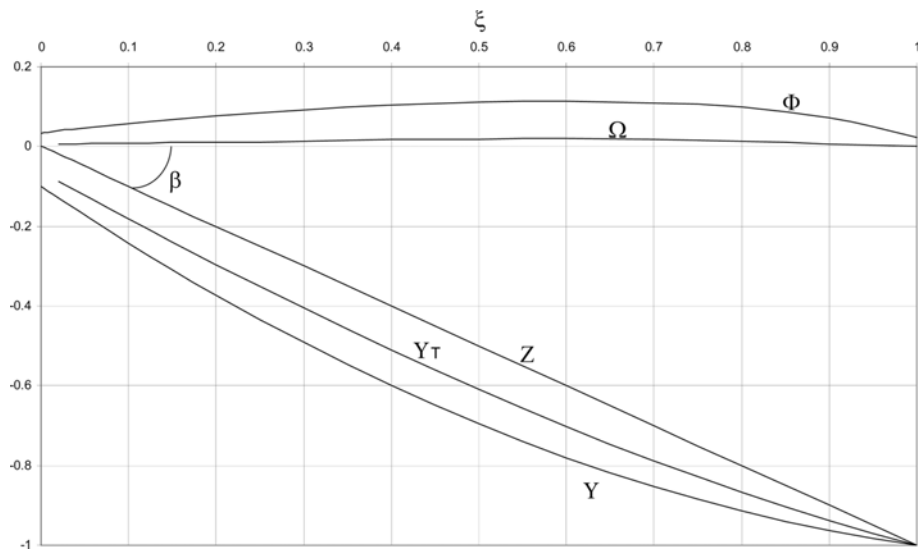
Fig. 16 Thrust force and normal stress distributions corresponding to the minimum value of a safety factor, the slope angle inclination $\beta = 45°$

One of the existing approaches to analyze slope stability considers the slip mass as a whole and assumes that the normal stress distribution along the slip line is a quadratic curve (Yang *et al.* 2001). It is interesting to compare values of the factor of safety (Yang *et al.* 2001) with the minimum values obtained by the present method for several slopes. The slope properties are the following: the height is 20 meters, the soil unit weight is 17.66 kN/m^3, the internal friction angle is 20°, and the cohesion is 9.81 kPa. The non-dimensional depth of the vertical crack at the top of the slope is $Y_0 - Z_0 = 0.1$. The minimum factors of safety for the slopes with initial inclination angles

$25°$ and $45°$ that were obtained by the present method are $F_{25} = 1.52$ and $F_{45} = 0.775$. (Note, that a slope with $F < 1$ is unstable). The corresponding values obtained by Yang *et al.* are $F_{25} = 1.9744$ and $F_{45} = 1.1301$. The plots of the slip and thrust lines, as well as distribution of the thrust force Ω and distribution of the normal stress along the slip line ($\Phi = \sigma_e/\gamma L$) for the slopes with initial inclination angles $25°$ and $45°$ are shown in Figs. 15-16, respectively.

6. Conclusions

A method for slope stability analysis, which is based on the coupled approximation of the slip and thrust lines is presented. The differential equation describing the thrust force distribution has been derived. It is based on subdivision of the sliding mass into differential slices, normal to the slip line, and applying the equilibrium requirements. Analysis of the equilibrium equation shows that the slide line can start only from a point, located within the sliding mass at some distance below the slope top surface. Therefore an initial crack at the top of the sliding mass is necessary to initiate the slide process. A thrust line within the soil mass above the trial slip line excludes the possible development of tension between slices in the stable and critical states. The coordinates of the thrust line upper boundary point are obtained by equilibrium of the upper triangular slice. Contrary to the conventional iterative limit equilibrium procedure, the factor of safety in the present method is prescribed in advance to ensure the slope reliability, and then the slope stability is checked for the given slip and thrust lines. Slope stability analysis is based on a numerical solution of the above mentioned equation and on the analysis of the thrust force at the slip line endpoint. The present method is applicable to any smooth shape of the slip line. For the above numerical examples, this shape was chosen as a quadratic parabola. The analysis of several slopes that were considered previously by other authors has been carried out utilizing the present method and comparison of the obtained results demonstrates the present method correctness and physically significance.

References

Bishop, A.W. (1955), "The use of the slip circle in stability analysis of slopes", *Geotechnique*, **5**(1), 7-17.

Fellenius, W. (1936), "Calculation of the stability of earth dams", *Proc. 2nd Congress on Large Dams*, **4**, 445-462.

Ginzburg, L. and Razdolsky, A. (1992), "Determination of maximum sliding soil pressure", *osnovaniya, fundamenty i mekhanika gruntov*, **5**, 11-14 (in Russian).

Janbu, N. (1954), "Application of composite slip surface for stability analysis", *Proc. of European Conference on Stability of Earth Slopes*, Stockholm, **3**, 43-49.

Janbu, N. (1973), "Slope stability computations. Embankment-dam engineering", Casagrande Volume, R.C. Hirschfeld and S.S. Poulos, eds., John Wiley and Sons, N.Y., 47-86.

Leshchinsky, D. (1990), "Slope stability analysis: generalized approach", *J. Geotechnical Engrg.*, ASCE, **118**(10), 851-867.

Morgenstern, N.R. and Price, V.E. (1965), "The analysis of the stability of general slip surfaces", *Geotechnique*, **15**(1), 70-93.

Sharma, S. and Moudud, A. (1992), "Interactive slope analysis using Spencer's method", *Proc. Spec. Conference on Stability and Performance of Slopes and Embankments-II*, ASCE, **1**, 506-520.

Spencer, E. (1973), "Thrust line criterion in embankment stability analysis", *Geotechnique*, **23**(1), 85-100.

Takuo, Y., Jing-Cai, J. and Katsutoshi, U. (2000), "Limit equilibrium stability analysis of slopes with stabilizing

piles", *Geotechnical Special Publication*. No.101, ASCE, 343-354.

Yang, H., Wang, J. and Liu, Y. (2001), "A new approach for the slope stability analysis", *Mech. Research Communications*, **28**(6), 653-669.

Zhu, D.-Y. and Qian, Q. (2000), "Determination of passive earth pressure coefficients by the method of triangular slices", *Canadian Geotechnical Journal*, **37**, 485-491.

Notation

c : cohesion with respect to the effective stress;

c_* : non-dimensional cohesion;

D : distance between the thrust and slip lines (length of vector $\boldsymbol{R}$ – see Fig. 1);

E : total lateral thrust on the side face of the slice (see Fig. 2);

F : factor of safety;

$h(x)$: equation of the slope line (external boundary of the slope cross section);

$H(x)$: equation of the potential slip line;

k : inclination of the slope line;

L : basic linear dimension;

$\boldsymbol{n}$: normal unit vector of the slip line (see Fig. 1);

r_u : pore water coefficient;

$\boldsymbol{R}$: vector that passes from the slip line to the thrust line;

s : line coordinate of the slice along the slip line (see Fig. 1);

t : tangent unit vectors on the slip line (see Fig. 1);

T : shear force on the side face of the slice (see Fig. 2);

u : pore water pressure (see Fig. 2);

V : height of the slice (see Fig. 1);

x, y : Cartesian coordinates;

Y, Z : non-dimensional coordinates of the slip and slope lines;

α : inclination of the slice base with respect to the horizontal axis (see Fig. 2);

φ : angle of shear resistance with respect to the effective stress;

Φ : non-dimensional effective normal stress;

γ : unit weight of the soil;

ΔW : weight of the slice (see Fig. 2);

Λ : non-dimensional length of the vector $\boldsymbol{R}$;

θ_0 : initial angle of the line $\Lambda(\xi)$ inclination;

ρ : radius of curvature of the slip line;

σ_e : effective normal stress at the bottom of a slice (see Fig. 2);

τ : shear stress at the bottom of the slice (see Fig. 2);

Ω : non-dimensional total lateral thrust;

ξ : non-dimensional linear coordinate.

Appendix: Interim transformations preceeding the equilibrium Eqs. (6)-(7)

The Eqs. (6)-(7) is derived from Eqs. (1)-(2) as a result of the follows transformations:

$$\sum_n = \left(T\left(s - \frac{\delta s}{2}\right), \boldsymbol{n}\right) + \left(E\left(s - \frac{\delta s}{2}\right), \boldsymbol{n}\right) + (\Delta W, \boldsymbol{n}) - \left(T\left(s + \frac{\delta s}{2}\right), \boldsymbol{n}\right) -$$

$$-\left(E\left(s + \frac{\delta s}{2}\right), \boldsymbol{n}\right) + \int_{s - \frac{\delta s}{2}}^{s + \frac{\delta s}{2}} [((\sigma_e + u)\boldsymbol{n}, \boldsymbol{n}) + (\tau t, \boldsymbol{n})]ds = 0$$

where notation $(\boldsymbol{a}, \boldsymbol{b})$ shows a scalar product of vectors $\boldsymbol{a}$ and $\boldsymbol{b}$

$$\boldsymbol{E}\left(s \pm \frac{\delta s}{2}\right) = \boldsymbol{E}(s) \pm \frac{d\boldsymbol{E}}{ds}\frac{\delta s}{2} = \boldsymbol{E}(s) \pm \left(\frac{d E}{ds}\boldsymbol{t} + E\frac{d\boldsymbol{t}}{ds}\right)\frac{\delta s}{2}$$

$$\boldsymbol{T}\left(s \pm \frac{\delta s}{2}\right) = \boldsymbol{T}(s) \pm \frac{d\boldsymbol{T}}{ds}\frac{\delta s}{2} = \boldsymbol{T}(s) \mp \left(\frac{d T}{ds}\boldsymbol{n} + T\frac{d\boldsymbol{n}}{ds}\right)\frac{\delta s}{2}$$

$$\sum_n = (\boldsymbol{T}(s), \boldsymbol{n}) + \left[\frac{dT}{ds}(\boldsymbol{n}, \boldsymbol{n}) + T\left(\frac{d\boldsymbol{n}}{ds}, \boldsymbol{n}\right)\right]\frac{\delta s}{2} + (\boldsymbol{E}(s), \boldsymbol{n}) -$$

$$-\left[\frac{dE}{ds}(\boldsymbol{t}, \boldsymbol{n}) + E\left(\frac{d\boldsymbol{t}}{ds}, \boldsymbol{n}\right)\right]\frac{\delta s}{2} + \Delta W[(\boldsymbol{t}, \boldsymbol{n})\sin\alpha - (\boldsymbol{n}, \boldsymbol{n})\cos\alpha] - (\boldsymbol{T}(s), \boldsymbol{n}) +$$

$$+\left[\frac{dT}{ds}(\boldsymbol{n}, \boldsymbol{n}) + T\left(\frac{d\boldsymbol{n}}{ds}, \boldsymbol{n}\right)\right]\frac{\delta s}{2} - (\boldsymbol{E}(s), \boldsymbol{n}) - \left[\frac{dE}{ds}(\boldsymbol{t}, \boldsymbol{n}) + E\left(\frac{d\boldsymbol{t}}{ds}, \boldsymbol{n}\right)\right]\frac{\delta s}{2} +$$

$$+ \int_{s-\frac{\delta s}{2}}^{s+\frac{\delta s}{2}} [((\sigma_e + u)\boldsymbol{n}, \boldsymbol{n}) + (\tau\boldsymbol{t}, \boldsymbol{n})]ds = 0$$

$$\sum_n = \left[\frac{dT}{ds}(\boldsymbol{n}, \boldsymbol{n}) + T\left(\frac{d\boldsymbol{n}}{ds}, \boldsymbol{n}\right)\right]\delta s - \left[\frac{dE}{ds}(\boldsymbol{t}, \boldsymbol{n}) + E\left(\frac{d\boldsymbol{t}}{ds}, \boldsymbol{n}\right)\right]\delta s +$$

$$+ \Delta W[(\boldsymbol{t}, \boldsymbol{n})\sin\alpha - (\boldsymbol{n}, \boldsymbol{n})\cos\alpha] + [(\sigma_e + u)(\boldsymbol{n}, \boldsymbol{n}) + \tau(\boldsymbol{t}, \boldsymbol{n})]_* \delta s = 0$$

$$\lim_{\delta s \to 0} \frac{\sum_n}{\delta s} = \left[\frac{dT}{ds}(\boldsymbol{n}, \boldsymbol{n}) + T\left(\frac{d\boldsymbol{n}}{ds}, \boldsymbol{n}\right)\right] - \left[\frac{dE}{ds}(\boldsymbol{t}, \boldsymbol{n}) + E\left(\frac{d\boldsymbol{t}}{ds}, \boldsymbol{n}\right)\right] +$$

$$+ \lim_{\delta s \to 0} \frac{\Delta W}{\delta s}[(\boldsymbol{t}, \boldsymbol{n})\sin\alpha - (\boldsymbol{n}, \boldsymbol{n})\cos\alpha] + (\sigma_e + u)(\boldsymbol{n}, \boldsymbol{n}) + \tau(\boldsymbol{t}, \boldsymbol{n}) = 0$$

$$\frac{d\boldsymbol{t}}{ds} = -\frac{1}{\rho}\boldsymbol{n}, \qquad \frac{d\boldsymbol{n}}{ds} = \frac{1}{\rho}\boldsymbol{t}$$

$$\frac{dT}{ds}(\boldsymbol{n}, \boldsymbol{n}) - \frac{1}{\rho}T(\boldsymbol{t}, \boldsymbol{n}) - \frac{dE}{ds}(\boldsymbol{t}, \boldsymbol{n}) + \frac{1}{\rho}E(\boldsymbol{n}, \boldsymbol{n}) +$$

$$+ \frac{dW}{ds}[(\boldsymbol{t}, \boldsymbol{n})\sin\alpha - (\boldsymbol{n}, \boldsymbol{n})\cos\alpha] + (\sigma_e + u)(\boldsymbol{n}, \boldsymbol{n}) + \tau(\boldsymbol{t}, \boldsymbol{n}) = 0$$

$$\frac{dT}{ds}(\boldsymbol{n}, \boldsymbol{n}) + \frac{1}{\rho}E(\boldsymbol{n}, \boldsymbol{n}) - \frac{dW}{ds}(\boldsymbol{n}, \boldsymbol{n})\cos\alpha + (\sigma_e + u)(\boldsymbol{n}, \boldsymbol{n}) = 0$$

$$\sigma_e + u = \frac{dW}{ds}\cos\alpha - \frac{dT}{ds} - \frac{1}{\rho}E$$

$$\sum_t = \left(\boldsymbol{T}\left(s - \frac{\delta s}{2}\right), \boldsymbol{t}\right) + \left(\boldsymbol{E}\left(s - \frac{\delta s}{2}\right), \boldsymbol{t}\right) + (\Delta W, \boldsymbol{t}) - \left(\boldsymbol{T}\left(s + \frac{\delta s}{2}\right), \boldsymbol{t}\right) -$$

$$- \left(\boldsymbol{E}\left(s + \frac{\delta s}{2}\right), \boldsymbol{t}\right) + \int_{s-\frac{\delta s}{2}}^{s+\frac{\delta s}{2}} [((\sigma_e + u)\boldsymbol{n}, \boldsymbol{t}) + (\tau\boldsymbol{t}, \boldsymbol{t})]ds = 0$$

$$\sum_t = (\boldsymbol{T}(s), \boldsymbol{t}) + \left[\frac{dT}{ds}(\boldsymbol{n}, \boldsymbol{t}) + T\left(\frac{d\boldsymbol{n}}{ds}, \boldsymbol{t}\right)\right]\frac{\delta s}{2} + (\boldsymbol{E}(s), \boldsymbol{t}) -$$

$$-\left[\frac{dE}{ds}(\boldsymbol{t}, \boldsymbol{t}) + E\left(\frac{d\boldsymbol{t}}{ds}, \boldsymbol{t}\right)\right]\frac{\delta s}{2} + \Delta W[(\boldsymbol{t}, \boldsymbol{t})\sin\alpha - (\boldsymbol{n}, \boldsymbol{t})\cos\alpha] - (\boldsymbol{T}(s), \boldsymbol{t}) +$$

$$+\left[\frac{dT}{ds}(\boldsymbol{n}, \boldsymbol{t}) + T\left(\frac{d\boldsymbol{n}}{ds}, \boldsymbol{t}\right)\right]\frac{\delta s}{2} - (\boldsymbol{E}(s), \boldsymbol{t}) - \left[\frac{dE}{ds}(\boldsymbol{t}, \boldsymbol{t}) + E\left(\frac{d\boldsymbol{t}}{ds}, \boldsymbol{t}\right)\right]\frac{\delta s}{2} +$$

$$+ \int\limits_{s-\frac{\delta s}{2}}^{s+\frac{\delta s}{2}} [((\sigma_e + u)\boldsymbol{n}, \boldsymbol{t}) + (\tau\boldsymbol{t}, \boldsymbol{t})]ds = 0$$

$$\lim_{\delta s \to 0} \frac{\sum_t}{\delta s} = \left[\frac{dT}{ds}(\boldsymbol{n}, \boldsymbol{t}) + T\left(\frac{d\boldsymbol{n}}{ds}, \boldsymbol{t}\right)\right] - \left[\frac{dE}{ds}(\boldsymbol{t}, \boldsymbol{t}) + E\left(\frac{d\boldsymbol{t}}{ds}, \boldsymbol{t}\right)\right] +$$

$$+ \lim_{\delta s \to 0} \frac{\Delta W}{\delta s}[(\boldsymbol{t}, \boldsymbol{t})\sin\alpha - (\boldsymbol{n}, \boldsymbol{t})\cos\alpha] + (\sigma_e + u)(\boldsymbol{n}, \boldsymbol{t}) + \tau(\boldsymbol{t}, \boldsymbol{t}) = 0$$

$$\frac{dT}{ds}(\boldsymbol{n}, \boldsymbol{t}) + \frac{1}{\rho}T(\boldsymbol{t}, \boldsymbol{t}) - \frac{dE}{ds}(\boldsymbol{t}, \boldsymbol{t}) + \frac{1}{\rho}E(\boldsymbol{n}, \boldsymbol{t}) +$$

$$+ \frac{dW}{ds}[(\boldsymbol{t}, \boldsymbol{t})\sin\alpha - (\boldsymbol{n}, \boldsymbol{t})\cos\alpha] + (\sigma_e + u)(\boldsymbol{n}, \boldsymbol{t}) + \tau(\boldsymbol{t}, \boldsymbol{t}) = 0$$

$$\frac{1}{\rho}T - \frac{dE}{ds} + \frac{dW}{ds}\sin\alpha + \tau = 0$$

$$\tau = -\frac{1}{F}(c + \sigma_e\tan\varphi), \qquad \sigma_e = \frac{dW}{ds}\cos\alpha - \frac{dT}{ds} - \frac{1}{\rho}E - u, \qquad \frac{dW}{ds} = \gamma V$$

$$\frac{1}{\rho}T = \frac{dE}{ds} - \gamma V\sin\alpha + \frac{1}{F}(c + \sigma_e\tan\varphi)$$

$$\frac{1}{\rho}T = \frac{dE}{ds} - \gamma V\sin\alpha + \frac{1}{F}\left[c + \left(\gamma V\cos\alpha - \frac{dT}{ds} - \frac{1}{\rho}E - u\right)\tan\varphi\right]$$

$$\frac{dE}{ds} = \gamma V\left(\sin\alpha - \frac{1}{F}\cos\alpha\tan\varphi\right) + \frac{1}{F}\frac{E}{\rho}\tan\varphi + \frac{T}{\rho} -$$

$$+ \frac{1}{F}\frac{dT}{ds}\tan\varphi - \frac{1}{F}(c - u\tan\varphi)$$

$$\sum M = \left[\boldsymbol{R}\left(s - \frac{\delta s}{2}\right) - \frac{\delta s}{2}\boldsymbol{t}\right] \times \boldsymbol{E}\left(s - \frac{\delta s}{2}\right) - \left[\boldsymbol{R}\left(s + \frac{\delta s}{2}\right) + \frac{\delta s}{2}\boldsymbol{t}\right] \times \boldsymbol{E}\left(s + \frac{\delta s}{2}\right) -$$

$$- \frac{\delta s}{2}\boldsymbol{t} \times \boldsymbol{T}\left(s - \frac{\delta s}{2}\right) - \frac{\delta s}{2}\boldsymbol{t} \times \boldsymbol{T}\left(s + \frac{\delta s}{2}\right) + \frac{V}{2}\boldsymbol{n} \times \Delta W = 0$$

$$\boldsymbol{R}\left(s \pm \frac{\delta s}{2}\right) \pm \frac{\delta s}{2}\boldsymbol{t} = \boldsymbol{R}(s) \pm \frac{d\boldsymbol{R}}{ds}\frac{\delta s}{2} \pm \frac{\delta s}{2}\boldsymbol{t} = \boldsymbol{R}(s) \pm \left(\boldsymbol{n}\frac{dD}{ds} + D\frac{d\boldsymbol{n}}{ds} + \boldsymbol{t}\right)\frac{\delta s}{2}$$

$$\sum M = \left[\boldsymbol{R}(s) - \left(\boldsymbol{n}\frac{dD}{ds} + D\frac{d\boldsymbol{n}}{ds} + \boldsymbol{t} \right)\frac{\delta s}{2} \right] \times \left[\boldsymbol{E}(s) - \left(\frac{dE}{ds}\boldsymbol{t} + E\frac{d\boldsymbol{t}}{ds} \right)\frac{\delta s}{2} \right] -$$

$$- \left[\boldsymbol{R}(s) + \left(\boldsymbol{n}\frac{dD}{ds} + D\frac{d\boldsymbol{n}}{ds} + \boldsymbol{t} \right)\frac{\delta s}{2} \right] \times \left[\boldsymbol{E}(s) + \left(\frac{dE}{ds}\boldsymbol{t} + E\frac{d\boldsymbol{t}}{ds} \right)\frac{\delta s}{2} \right] -$$

$$- \frac{\delta s}{2}\boldsymbol{t} \times \left[\boldsymbol{T}(s) + \left(\boldsymbol{n}\frac{dT}{ds} + T\frac{d\boldsymbol{n}}{ds} \right)\frac{\delta s}{2} \right] - \frac{\delta s}{2}\boldsymbol{t} \times \left[\boldsymbol{T}(s) - \left(\boldsymbol{n}\frac{dT}{ds} + T\frac{d\boldsymbol{n}}{ds} \right)\frac{\delta s}{2} \right] + \frac{V}{2}\boldsymbol{n} \times \Delta\boldsymbol{W} = 0$$

$$\boldsymbol{R}(s) \times \boldsymbol{E}(s) - \left(\boldsymbol{n}\frac{dD}{ds} + D\frac{d\boldsymbol{n}}{ds} + \boldsymbol{t} \right)\frac{\delta s}{2} \times \boldsymbol{E}(s) - \boldsymbol{R}(s) \times \left(\frac{dE}{ds}\boldsymbol{t} + E\frac{d\boldsymbol{t}}{ds} \right)\frac{\delta s}{2} +$$

$$+ \left(\boldsymbol{n}\frac{dD}{ds} + D\frac{d\boldsymbol{n}}{ds} + \boldsymbol{t} \right)\frac{\delta s}{2} \times \left(\frac{dE}{ds}\boldsymbol{t} + E\frac{d\boldsymbol{t}}{ds} \right)\frac{\delta s}{2} - \boldsymbol{R}(s) \times \boldsymbol{E}(s) -$$

$$- \left(\boldsymbol{n}\frac{dD}{ds} + D\frac{d\boldsymbol{n}}{ds} + \boldsymbol{t} \right)\frac{\delta s}{2} \times \boldsymbol{E}(s) - \boldsymbol{R}(s) \times \left(\frac{dE}{ds}\boldsymbol{t} + E\frac{d\boldsymbol{t}}{ds} \right)\frac{\delta s}{2} -$$

$$- \left(\boldsymbol{n}\frac{dD}{ds} + D\frac{d\boldsymbol{n}}{ds} + \boldsymbol{t} \right)\frac{\delta s}{2} \times \left(\frac{dE}{ds}\boldsymbol{t} + E\frac{d\boldsymbol{t}}{ds} \right)\frac{\delta s}{2} - \frac{\delta s}{2}\boldsymbol{t} \times \boldsymbol{T}(s) -$$

$$- \frac{\delta s}{2}\boldsymbol{t} \times \left(\boldsymbol{n}\frac{dT}{ds} + T\frac{d\boldsymbol{n}}{ds} \right)\frac{\delta s}{2} - \frac{\delta s}{2}\boldsymbol{t} \times \boldsymbol{T}(s) + \frac{\delta s}{2}\boldsymbol{t} \times \left(\boldsymbol{n}\frac{dT}{ds} + T\frac{d\boldsymbol{n}}{ds} \right)\frac{\delta s}{2} + \frac{V}{2}\boldsymbol{n} \times \Delta\boldsymbol{W} = 0$$

$$\left(\boldsymbol{n}\frac{dD}{ds} + D\frac{d\boldsymbol{n}}{ds} + \boldsymbol{t} \right) \times \boldsymbol{E}(s) + \boldsymbol{R}(s) \times \left(\frac{dE}{ds}\boldsymbol{t} + E\frac{d\boldsymbol{t}}{ds} \right) + \boldsymbol{t} \times \boldsymbol{T}(s) - \frac{V}{2}\boldsymbol{n} \times \frac{\Delta\boldsymbol{W}}{\delta s} = 0$$

$$\left(\boldsymbol{n}\frac{dD}{ds} + D\frac{d\boldsymbol{n}}{ds} + \boldsymbol{t} \right) \times E\boldsymbol{t} + D\boldsymbol{n} \times \left(\frac{dE}{ds}\boldsymbol{t} + E\frac{d\boldsymbol{t}}{ds} \right) - \boldsymbol{t} \times T\boldsymbol{n} + \frac{V}{2}\frac{dW}{ds}(\boldsymbol{n} \times \cos\alpha\,\boldsymbol{n} - \boldsymbol{n} \times \sin\alpha\,\boldsymbol{t}) = 0$$

$$\left(\boldsymbol{n}\frac{dD}{ds} + D\frac{d\boldsymbol{n}}{ds} + \boldsymbol{t} \right) \times E\boldsymbol{t} + D\boldsymbol{n} \times \left(\frac{dE}{ds}\boldsymbol{t} + E\frac{d\boldsymbol{t}}{ds} \right) - \boldsymbol{t} \times T\boldsymbol{n} + \gamma\frac{V^2}{2}[\cos\alpha(\boldsymbol{n} \times \boldsymbol{n}) - \sin\alpha(\boldsymbol{n} \times \boldsymbol{t})] = 0$$

$$E\frac{dD}{ds}(\boldsymbol{n} \times \boldsymbol{t}) + \frac{1}{\rho}ED(\boldsymbol{t} \times \boldsymbol{t}) + E(\boldsymbol{t} \times \boldsymbol{t}) + D\frac{dE}{ds}(\boldsymbol{n} \times \boldsymbol{t}) - DE\frac{1}{\rho}(\boldsymbol{n} \times \boldsymbol{n}) -$$

$$- T(\boldsymbol{t} \times \boldsymbol{n}) + \gamma\frac{V^2}{2}[\cos\alpha(\boldsymbol{n} \times \boldsymbol{n}) - \sin\alpha(\boldsymbol{n} \times \boldsymbol{t})] = 0$$

$$- E\frac{dD}{ds} - D\frac{dE}{ds} - T + \gamma\frac{V^2}{2}\sin\alpha = 0$$

$$T = \gamma\frac{V^2}{2}\sin\alpha - E\frac{dD}{ds} - D\frac{dE}{ds}$$